

# Influence of the atmosphere model and the quality of the ballistic coefficient (BC) estimation on the prediction of the re-entry moment

**Mikołaj Krużyński, Zygmunt Anioł, Krzysztof Armiński, Dorota Mieczkowska, Marcin Teofilewicz, Edwin Wnuk, Tomasz Zubowicz**

*Polish Space Agency*

**Justyna Gołębiowska, Monika K. Kamińska, Krzysztof Kamiński, Dorota Krużyńska, Julia Pietrzak**

*Astronomical Observatory Institute, Faculty of Physics, A. Mickiewicz University, Poznan*

**Marek Poleski**

*Faculty of Power and Aeronautical Engineering, Warsaw University of Technology*

## ABSTRACT

This paper presents results of a research work on the influence of two fundamental factors on re-entry event modeling: atmosphere model and ballistic coefficient. During the work, astrometric observations of three satellites were made during a 10-day observation campaign. Then, a re-entry analysis was performed, predicting the moment of re-entry into the atmosphere. As part of the analysis, the impact of different models of the atmosphere was compared and four different methods of estimating the value of the ballistic coefficient were presented, and then they were used in the analysis of the observed satellites. By comparing the methods, the predicted moments of re-entry were calculated. On this basis, the usefulness of individual methods and the conditions of applicability were determined.

## 1. INTRODUCTION

The number of satellites orbiting the Earth is still increasing. Also, an increase in the number of decaying objects is observed as indicated in Fig. 1. In fact, dozens of decays are observed every year and almost 30,000 objects have entered the atmosphere since the beginning of the space era. Most of those objects will burn up during re-entry, but not all of them. Objects of large size and mass can survive entering the atmosphere. With that in mind, a decaying satellite object may pose a threat to both people and infrastructure. Therefore, monitoring and predicting the moment of decay is important to mitigate the possible risk of incidents with the general population and infrastructure located on the ground.

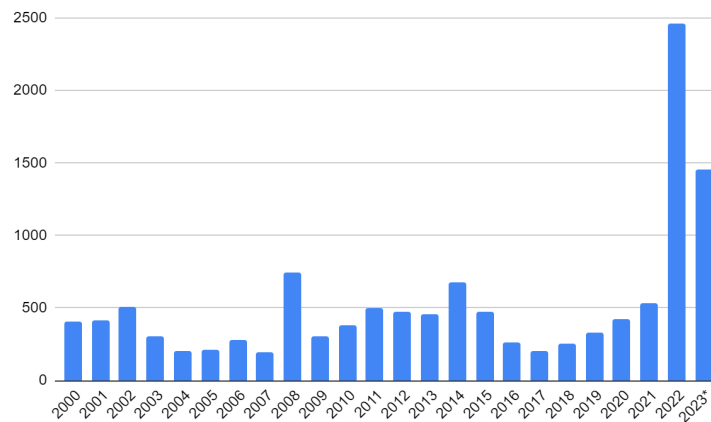


Fig. 1. Number of decays in the years 2000-2023.

This is a challenging task due to various phenomena acting on decaying objects. These are represented by the perturbing forces and result in increase in the structural complexity of the algorithms used. This complexity is the result of advanced models required to describe these phenomena. In addition, the use of such models requires the

identification of a significant number of parameters, which is also reflected in the difficulty of the problem. Hence, the inherent property of the problem is that it is subject to elevated levels of uncertainty. This becomes all the more significant in the case of low orbits, where there is a significant increase in the number of factors affecting the object's motion - such as the influence of the atmosphere, for example. Also, it is this factor, which is the source of the significant level of uncertainty influencing the predicted moment of decay. Indeed, the factor identified as resulting in the highest level of uncertainty is the atmospheric drag, which typically aggregates limited knowledge about the state of the atmosphere. This is further elaborated in the following paragraph.

Modeling the drag (perturbing) force is difficult due to two main reasons. First, a reliable forecast of the dynamic state of the atmosphere is required. This is a difficult task due to spatial distribution of the model and limited number of measurements. Second, an exact characteristic of the physical properties of the object entering the atmosphere is needed. These, however, may change due to the interaction of object and atmosphere during decay and there is no technologically feasible manner to directly observe or measure the phenomenon. The factors which are of most interest to the problem include object mass, cross-sectional area, drag coefficient depending on the shape and material of which the satellite is made, make up the value of the ballistic coefficient (BC). Unfortunately, the last value is difficult to estimate, and the estimate is prone to aggregate the uncertainty resulting also from other sources or factors.

In practice, the problem of BC estimation is handled in various manners. Some typically used methods include:

- an approach based on the previously known physical characteristics of a decaying object. Known size and weight limit the range of BC values. However, such an approach may cause too much uncertainty in the case of objects with an irregular shape and a large span of individual dimensions. In addition, this approach is impossible to apply to objects whose dimensions are unknown a priori, e.g. objects resulting from fragmentation;
- the use of data contained in the orbital catalog space-track.org. In the orbital catalog saved in the TLE format, the coefficient  $B^*$  is included. After making appropriate calculations, it is possible to estimate the BC;
- method based on the historical orbital elements of the object. Using proprietary in-house software, the average BC was determined and the prediction of the decay moment of selected objects was performed;
- an approach to determine the parameter during the orbit determination process by including this parameter in the state vector. We used the Kalman filter and least square methods in our calculations. This approach allows for determining the instantaneous BC, but it can be used only when we have a sufficiently large number of observations.

Each of these approaches has its limitations. In this work, the applicability of individual approaches and the results obtained in each of them were verified. The analysis was carried out for objects that have re-entered the atmosphere in recent years and compared. As a result, information was obtained on the impact of the atmospheric models used and the effectiveness of individual BC estimation methods on the quality of prediction of the moment of re-entry.

## 2. ATMOSPHERE MODELING/INFLUENCE

Many approaches exist that consider atmospheric density modeling. Popular atmospheric models include, among many others, Jacchia, DTM and MSIS, as well as their variations and versions [1, 2, 5]. Although physical models are available, it is the empirical ones that are currently in operational use more often [1, 3]. The density predictions provided by these empirical models can differ by 30% between each other, which probably, among other factors, can be traced back to having not enough data gathered by measuring instruments. Also, the data can differ by about 30% between measurements from the same instrument as well [2].

In Fig. 2, a comparison in satellite propagation between four selected models: DTM, Jacchia-Roberts, MSISE and NRLMSISE00 is presented for three Low Earth Orbit objects: COSMOS 1356 (NORAD ID 13153), COSMOS 1408 DEB (NORAD ID 49524) and STARLINK-1125 (NORAD ID 44950). In this comparison, each propagation was started 7 days before re-entry. Each calculation starts from the same initial state, with the same force model and differs only in terms of the atmosphere model. All objects were assumed to be spherical and to have a drag coefficient of 2.2. Orbits were propagated to an altitude of 100 km, except DTM which have model restrictions at 120 km. In this comparison, DTM model tends to predict the fastest orbit decay, while NRLMSISE00 seems to fall slightly slower. The comparison shows that it is important to take a precise model of the atmosphere in calculations,

especially when the re-entry case is analyzed. For low altitude objects, the impact of the atmosphere drag is really significant.

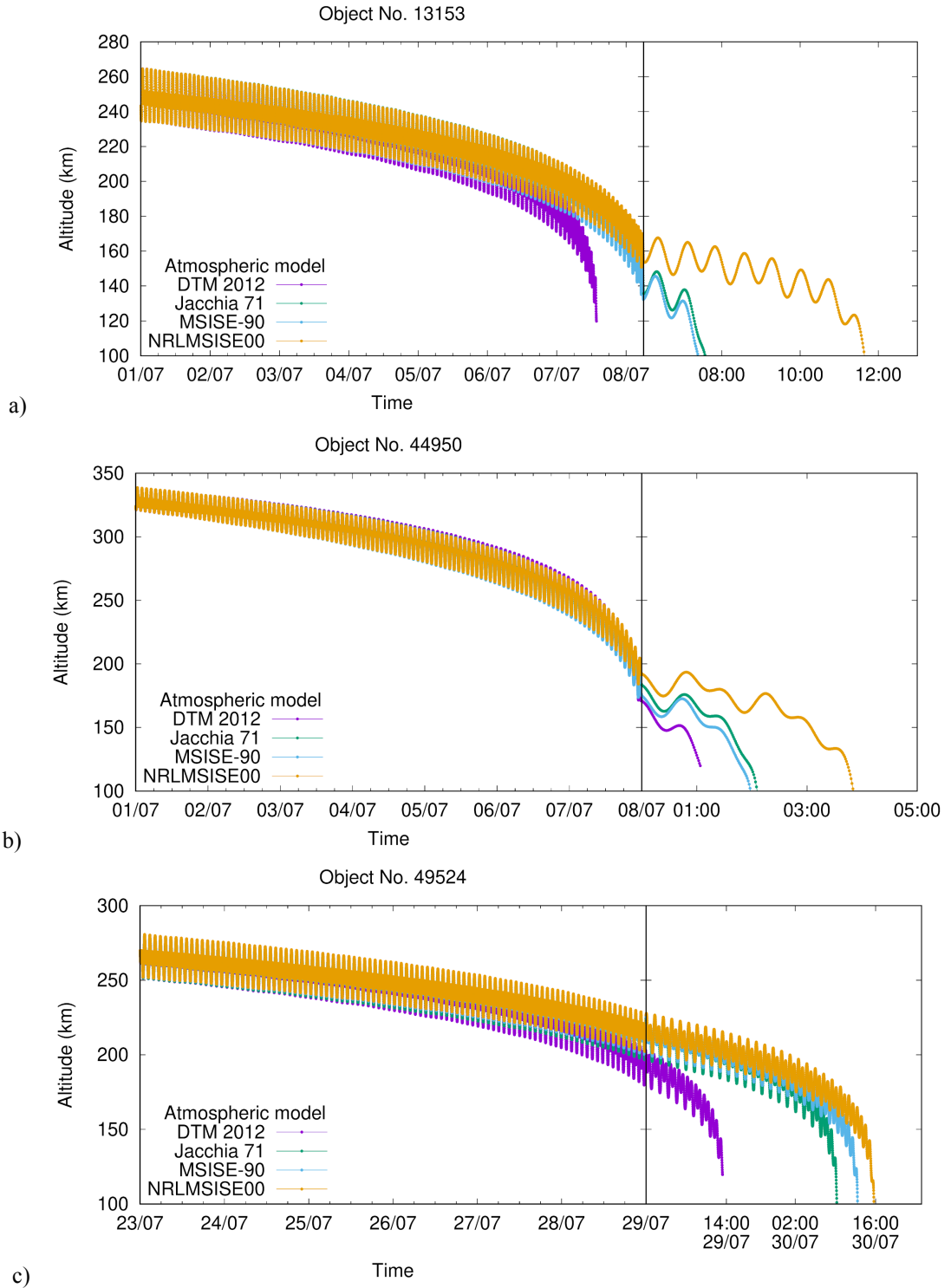


Fig. 2. Propagation for 7 days before re-entry with four different models of atmosphere for a) COSMOS 1356), b) STARLINK-1125, c) COSMOS 1408 DEB. On the right side of each plot timescale is zoomed to better present differences related to atmosphere model.

### 3. OBSERVATIONS

In the period from 1 to 12 June 2023, an observation campaign was performed during which satellite objects approaching re-entry were observed. Objects which re-entry was expected to take place within 30 - 60 days from the start of the campaign were selected. The observations were made using the PST3e sensor. It is a component of a cluster of telescopes located in Chalin, Poland belonging to the Adam Mickiewicz University, Poznań. PST3e is a 0.3-meter f/1.0 telescope with a fast direct-drive mount and sCMOS camera. It is dedicated to SST observations and has been used many times to observe objects on different orbital regimes, including Low Earth's Orbits [6,7]. Taking into account the requirements and limitations of the system, three objects were finally selected for the observations and further analysis. Information about chosen objects and observations statistics is included in Tab. 1.

Object	COSMOS 1356	STARLINK-1125	COSMOS 1408 DEB
Norad ID	13153	44950	49524
Cospar ID	1982-039A	2020-001AN	1982-092M
Launch epoch <sup>1</sup>	1982-05-05	2020-01-07	1982-09-16
Nominal re-entry epoch <sup>1</sup>	2023-07-08 04:48:00	2023-07-09 12:21:00	2023-07-30 21:10:00
Inclination	81.2 deg	53.1 deg	82.4 deg
Mass <sup>2</sup> [kg]	2477.7	260	N/A
Cross section <sup>2</sup>	Min [m <sup>2</sup> ]	1.327	N/A
	Avg [m <sup>2</sup> ]	8.068	N/A
	Max [m <sup>2</sup> ]	16.639	N/A
Number of passes	7	13	14
Number of observations	1719	4156	1703

Table 1. Summary of information about the observed satellites and observation campaign statistics.

### 4. BALLISTIC COEFFICIENT ESTIMATION

One of the most important parameters that must be taken into account when predicting the moment of re-entry is the ballistic coefficient ( $BC$ ). It is defined as:

$$BC = \frac{m}{C_d \cdot A} \quad (1)$$

where:

- $C_d$  is the drag coefficient, a parameter that considers the interaction of the atmosphere with the object;
- $A$  is the cross-sectional area of the object;
- $m$  is the mass of the object;

It describes the influence of the Earth's atmosphere on the satellite motion. In some studies, one can encounter an inverted value of this parameter. This should be taken into account when comparing the results obtained with different software.

Satellite lifetime is strongly correlated with  $BC$ . The larger the  $BC$ , the longer the satellite lifetime. Of course, for low satellites this proportion is even stronger. This relationship is presented in Fig. 3.

<sup>1</sup> <https://www.space-track.org/>

<sup>2</sup> <https://discosweb.esoc.esa.int/>

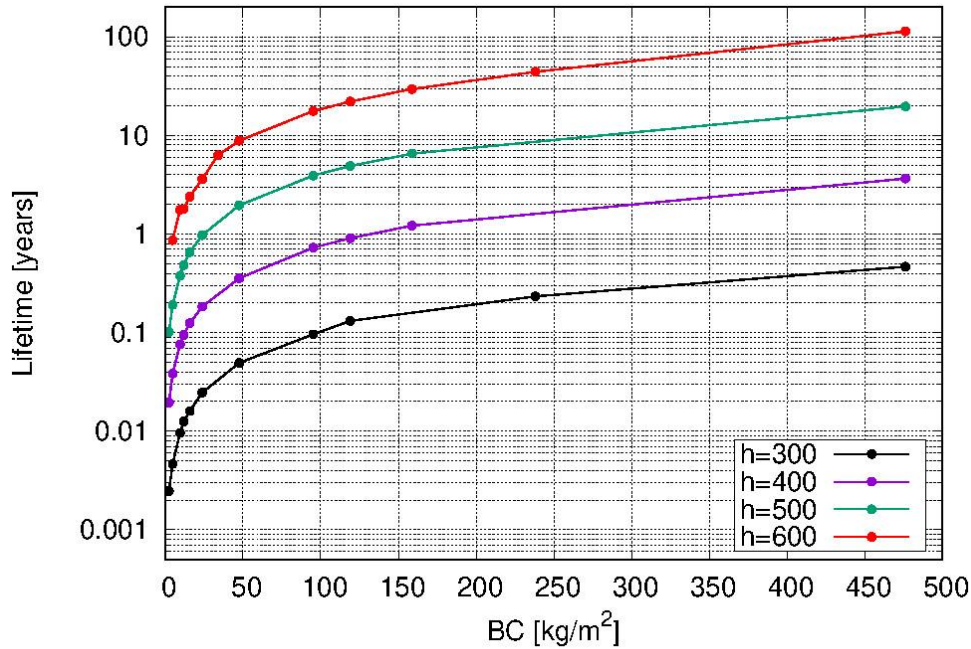


Fig. 3. Lifetime of objects in circular orbits at different heights ( $h=300\text{km}$ ,  $400\text{km}$ ,  $500\text{km}$ ,  $600\text{km}$ ) depending on the value of the ballistic coefficient [ $\text{kg}/\text{m}^2$ ].

Using various  $BC$  estimation methods, analyses were carried out to determine re-entry moments. Various commercial and in-house software tools were used. In most cases, the analysis was carried out taking into account the following forces:

- Earth's gravity: model egm2008, 70x70 order,
- third body gravity: Moon, Sun,
- atmosphere drag: model NRLMSISE-00,
- solar radiation pressure,
- solid tides.

#### 4.1 Physical properties of the object

One of the basic methods for determining  $BC$  is an estimation based on previously known physical parameters of the object. Sizes, materials used, weight and shape are perfectly known to the owner. Therefore, collecting such data in dedicated services can be very useful for such analyses of re-entry time estimation.

One of such databases is the service provided by ESA - Discos (<https://discosweb.esoc.esa.int/>). In it one can find information about the date and place of launching into orbit, the owner of the satellite, but also information about the satellite itself, such as size, mass and shape. There can be found the mass and 3 cross-sectional values: minimum, average and maximum. Based on these the three  $BC$  estimations per object can be calculated: min  $BC$ , avg  $BC$  and max  $BC$ . It is an excellent source of information to get any idea about the object we are dealing with.

The result of orbital propagation based on such calculation is presented in Fig. 4.

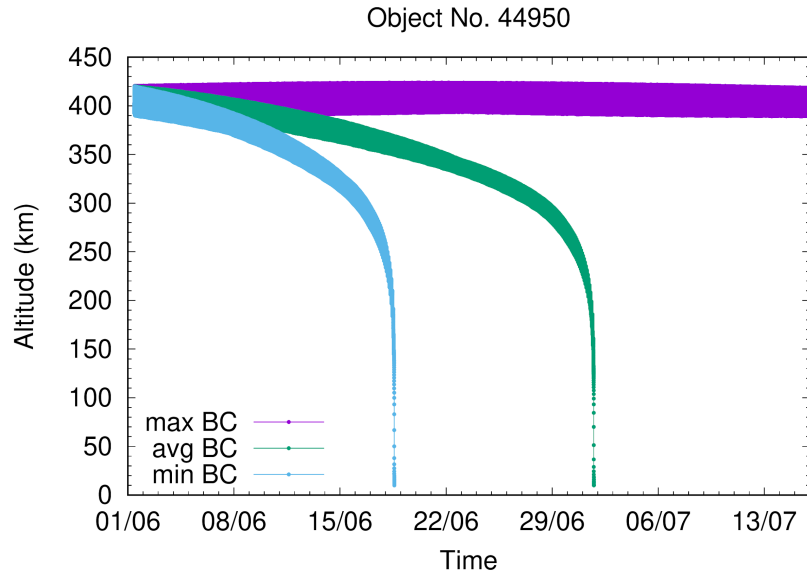


Fig. 4. STARLINK-1125 propagation for minimum, average and maximum  $BC$  estimated on the basis of previously known physical parameters.

It can be seen that the predicted moment of the reentry can differ substantially. Unfortunately, the use of these data directly does not give a clear answer regarding the expected date of the satellite's decay. Depending on the shape, the difference between the minimum and maximum cross section can vary by a factor of 100. In addition, necessary data in the database may be missing for some objects. In particular, objects resulting from fragmentation in orbit do not have specific physical parameters in the database. Based on available data,  $BC$  was determined and re-entry moments were determined for the minimum, average and maximum  $BC$ , respectively. Results are presented in Table 2.

Object		COSMOS 1356	STARLINK-1125	COSMOS 1408 DEB
Mass <sup>13</sup> [kg]		2477.7	260	N/A
Estimated $BC^1$	Min	67.69	5.00	N/A
	Avg	139.59	8.71	N/A
	Max	848.70	511.39	N/A
Estimated re-entry epoch	Min	2023-07-10 08:07	2023-06-18 14:02	N/A
	Avg	2023-09-15 05:34	2023-07-01 17:57	N/A
	Max	2024-12-16	2031-02-26	N/A
Nominal re-entry epoch <sup>2</sup>		2023-07-08 04:48:00	2023-07-09 12:21:00	2023-07-30 21:10:00

Table 2. Estimated  $BC$  and re-entry epoch based on physical parameters of objects available in Discos service.

#### 4.2 Ballistic coefficient and the $B^*$ coefficient

The easiest way to obtain the value of the ballistic coefficient from orbital data seems to be to use the  $B^*$  value from the catalog of orbits in TLE format. A simple formula for determining the ballistic coefficient with  $B^*$  is well known [12]:

$$BC = \frac{Re \rho}{2 B^*} \quad (2)$$

where  $\rho$  is the atmospheric density at perigee of the orbit and  $R_e$  is the radius of the Earth.

However, we should pay attention to the warning “the value of  $B^*$  is always modified. It's really an arbitrary free parameter in differential correction.” [12].

Values of ballistic coefficient for a given satellite object are not constant in time, mainly due to changes in the Earth atmosphere density  $r$  and different values of  $B^*$  in TLE elements for different epochs. Fig. 5 and Table 3 present results of ballistic coefficient analysis for three satellites taken into account in the present paper on a time span of one year before the re-entry epoch of these objects. Fig. 5 shows values of the  $BC$  obtained according to Eq. (4.2). The increase in values of  $BC$  is associated with a decrease in perigee and an increase in the density of the atmosphere. Table 3 contains minimum, maximum, median and average values of the ballistic coefficient  $BC$ . Some maximum values of  $BC$  reach very outlier values (not included in the Fig. 5), which are an example of the possibility of individual unreal  $BC$  values obtained by using Eq.2. Therefore, the use of single  $BC$  values obtained from  $B^*$  may result in errors in orbital propagation and in prediction of the re-entry moment. Values of the density  $\rho$  have been obtained from the NRLMSISE-00 model, using historical values of the geomagnetic planetary index and the solar flux (source: <https://celestrak.org/>).

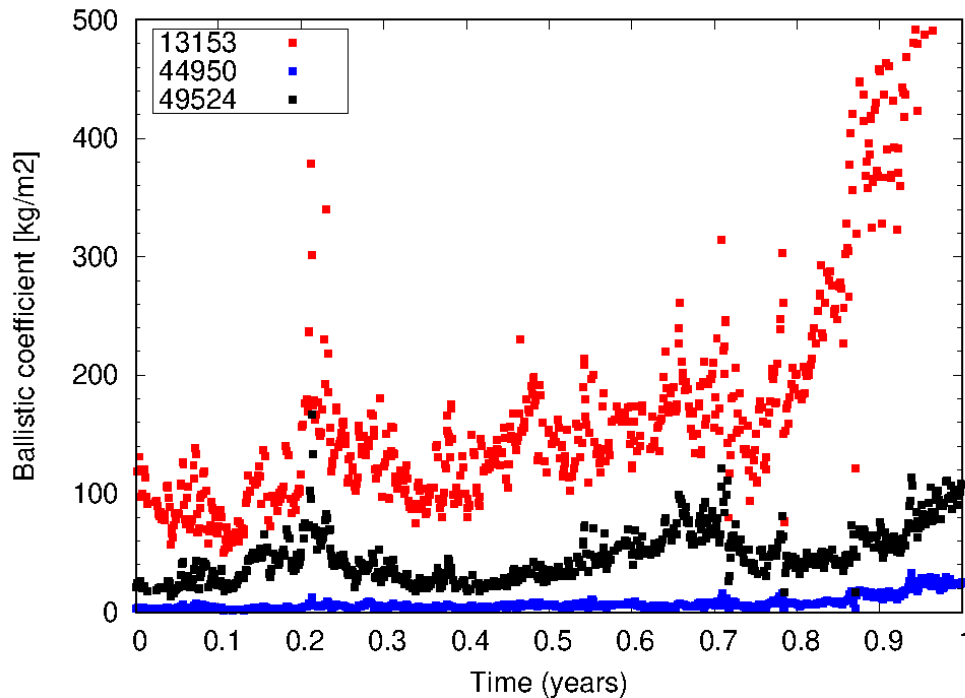


Fig. 5. BC estimation based on  $B^*$ .

Sat number	$BC$ min [ $\text{kg}/\text{m}^2$ ]	$BC$ max [ $\text{kg}/\text{m}^2$ ]	$BC$ average [ $\text{kg}/\text{m}^2$ ]	$BC$ median [ $\text{kg}/\text{m}^2$ ]
13153	50.23	716877.22	161.09	167.89
44950	1.63	30697.63	5.69	5.93
49524	16.43	2421.31	45.60	49.52

Table 3. BC estimation based on  $B^*$ .

The average value was obtained from the formula:

$$BC_A = \frac{\sum_{i=1}^n BC_i}{n} \quad (3)$$

Very outlier maximum values [not included in the graph] are an example of the possibility of obtaining individual unreal  $BC$  values in this method. Therefore, the use of single  $BC$  values obtained from  $B^*$  may result in errors in orbital propagation and prediction of the re-entry moment.

### 4.3 Method based on the historical orbital elements

The method of determination of ballistic coefficient  $BC$  value, that next is applied to re-entry prediction, presented below, is based only on NORAD TLE historical data for a given satellite object taken from the Satellite Catalog (space-track.org). The general idea of this method is rather simple: the decay epoch for a given object (time moment at which the object will reach a given altitude above the Earth ellipsoid, e.g. 80 km) is determined by orbital prediction starting from time epoch, initial conditions taken from TLE orbital elements at this epoch and the ballistic coefficient  $BC$  value obtained in a fitting process with the use of all TLE data from initial epoch to epoch before expected decay epoch.

The propagation of orbits in this method was performed using STOP – The Short-Term Orbit Propagator – software tool developed at the Astronomical Observatory of Adam Mickiewicz University [16]. The numerical version of STOP (with the use of numerical integration of equations of motion) has been used with the following force model: geopotential zonal and tesseral harmonic coefficients up to 30 degree and order, luni-solar effects, solar radiation pressure with cannonball modeling and including Earth’s shadow effects, atmospheric drag with NRLMSISE-00 model of the atmosphere, using historical values of the geomagnetic planetary index and the solar flux. These data were acquired from the Celestrak web page (<https://celestrak.org>). Initial conditions for the numerical integration have been obtained by transformation from mean TLE orbital elements at the epoch to osculating orbital elements with the use of algorithm presented in the paper [15].

Prediction of decay epoch of an object orbiting in the Earth’s atmosphere strongly depends on proper values of ballistic coefficient  $BC$  used in calculations of predicted trajectory of the object and of the Earth’s atmosphere density calculated from an applied atmospheric model with actual space weather data. Therefore, the most important part of the presented method is an estimation of the  $BC$  value with the highest possible accuracy. The ballistic coefficient average values obtained from  $B^*$  (Eq. 4.2) may be used only as the very preliminary estimation of this parameter and as the starting value in the fitting process that is used in the presented method. The accurate  $BC$  value at the epoch can be obtained by fitting the calculated predicted trajectory to trajectory described by the TLE Catalog orbital data [11].

The fitting method is based on the differential correction applied to historical TLE data. The catalog orbital data for given epochs are taken as “observations”  $O$ , and orbital elements calculated for these epochs with the use of the STOP orbit predictor are taken as “calculated values”  $C$ . Differential correction process adjusts the  $BC$  value by minimizing the residuals. In this method the orbital elements at the epoch are not corrected, however the applied fitting process takes into account also differences in semi-major axis (related to the orbital mean motion) between its values calculated from TLE “mean” mean motion and mean semi-major axis calculated from its osculating value obtained by the use of the STOP numerical propagator using transformation [15]. Therefore, the ballistic coefficient estimated in the presented fitting process includes also a part that is an influence of changes in the object’s orbital mean motion that should be included in the initial conditions at the epoch in the mean motion (or in semi-major axis) value as a correction. Because this correction is not included in the initial orbital elements, the ballistic coefficient determined by the presented method is not exactly the ratio between the cross-sectional area of the object and mass of the object as is defined by Eq. 1. Consequently, this value of the ballistic coefficient may be used only with the software tools presented in this paper and should not be applied in other orbital propagators.



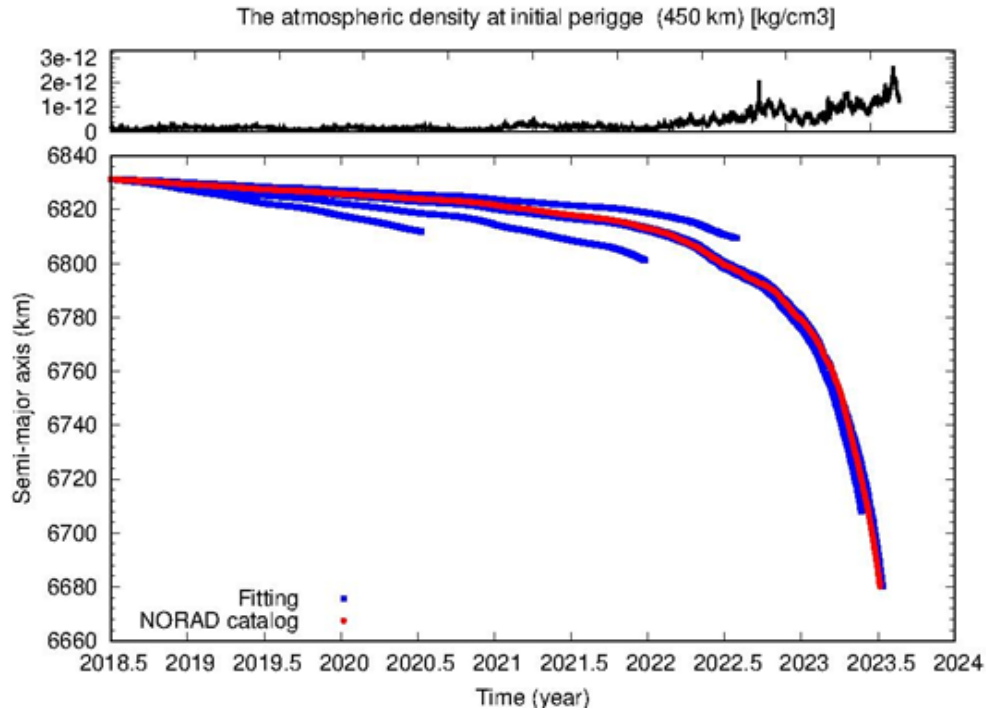


Fig. 6. Ballistic Coefficient fitting process for object NORAD 13153.

Exemplary results of the presented fitting process for the object NORAD 13153 with the use of TLE data taken for about 5 years are presented in Fig. 6. The red points show the semi-major axis values obtained from the TLE Catalog. The individual blue curves are the results of propagation with a specific  $BC$  value. The propagation stops when the difference between the observed (O) and calculated (C) values exceeds the predefined threshold. The fitting process ends when it manages to match the calculated values of the semimajor axis to all available values from the TLE Catalog. The top panel in Fig. 6 shows the atmospheric density at 450 km (perigee region). Comparing the time variations of the atmospheric density and changes of the semimajor axis it may be noted that an increase in density in 2022 caused the acceleration of the process of re-entry.

The final calculations of decay epoch for a given object are performed by the STOP tool, using its numerical version. Numerical integration of equations of motion starts with the following initial condition for the object: 1) osculating position and velocity obtained from TLE orbital elements at the epoch by the use of above-mentioned transformation [15], and 2) ballistic coefficient precisely determined in the fitting process.

The presented method of decay epoch determination based on historical TLE data is very effective and allows for precise prediction of this epoch. An example of application of this method for the satellite NORAD 13153 is presented on Fig. 7 a) and b). TLE data for this object has been used for the period from epoch 1 Feb. 2023 (23032) to epoch 10 June 2023 (23163). Applying the above presented fitting process, the value 53.1528 of ballistic coefficient for epoch was estimated. Next, STOP tool has been used for trajectory propagation from the epoch 10 June 2023 to decay epoch, which was 2023-07-08, 08:02:00. Satellite altitude  $h$  evolution during time span from 1 Feb. 2023 to estimated decay epoch is presented in Fig. 7 a) and last two days of this evolution are in Fig. 7 b). Note that the decay epoch predicted using the presented method is very close to the epoch predicted by 18 SDS and published by Space Track (space-track.org) two days before re-entry the decay epoch was 2023-07-08, 11:46:00 with window 600 min. Therefore, decay epoch predicted by the presented method with the initial conditions from the 1 Feb. 2023 (157 days before re-entry) and ballistic coefficient estimated on TLE data (determined from observations) ending at the 30 days before re-entry hits the decay epoch window determined by 18th SDS.

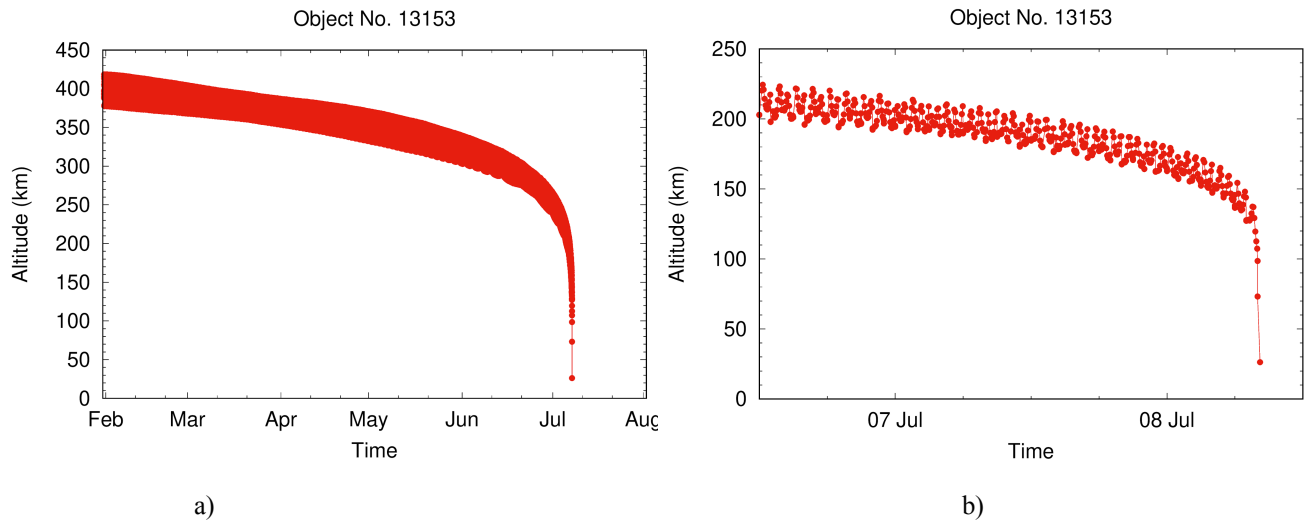


Fig. 7. Predicted altitude evolution before re-entry for COSMOS 1356..

According to the procedure described above, the value fitting process was carried out and then the re-entry moment was determined for other two objects: NORAD 44950 and NORAD 49524 with the accuracy very similar to results obtained for the object NORAD 13153.

Object	COSMOS 1356	STARLINK-1125	COSMOS 1408 DEB
Estimated $BC$	53.15	9.59	30.03
Estimated re-entry epoch	2023-07-08 08:02:58	2023-07-09 08:09:57	2023-07-30 22:49:24
Nominal re-entry epoch <sup>2</sup>	2023-07-08 04:48:00	2023-07-09 12:21:00	2023-07-30 21:10:00

Table 4. Estimated  $BC$  and re-entry epoch using method based on the historical orbital elements.

#### 4.4 Orbit determination

The process of correcting the orbits is an integral part of the analysis of the orbital motion of artificial Earth satellites. Routinely, the orbit should be updated based on current observations. The primary goal is to determine the current set of six elements describing the orbit. Observations made in the observation campaign contained information about the position of the satellite on the celestial sphere at various times and in the process the current orbit was determined. The orbit was calculated by combining several passes over the sensor. An observation arc that is too short does not give a sufficiently good precision of the determined orbit, while an observation arc that is too long may be impossible to recalculate to obtain a convergent solution. Therefore, the OD process needs to be properly controlled. An exemplary projection of the observed flights, which were recalculated in a single OD process, is shown in Fig. 8 a). Fig. 8 b) presents a plot of residuals over time in the declination and right ascension axes, respectively. It shows that the OD process is convergent and the quality of the individual measurements is very good.

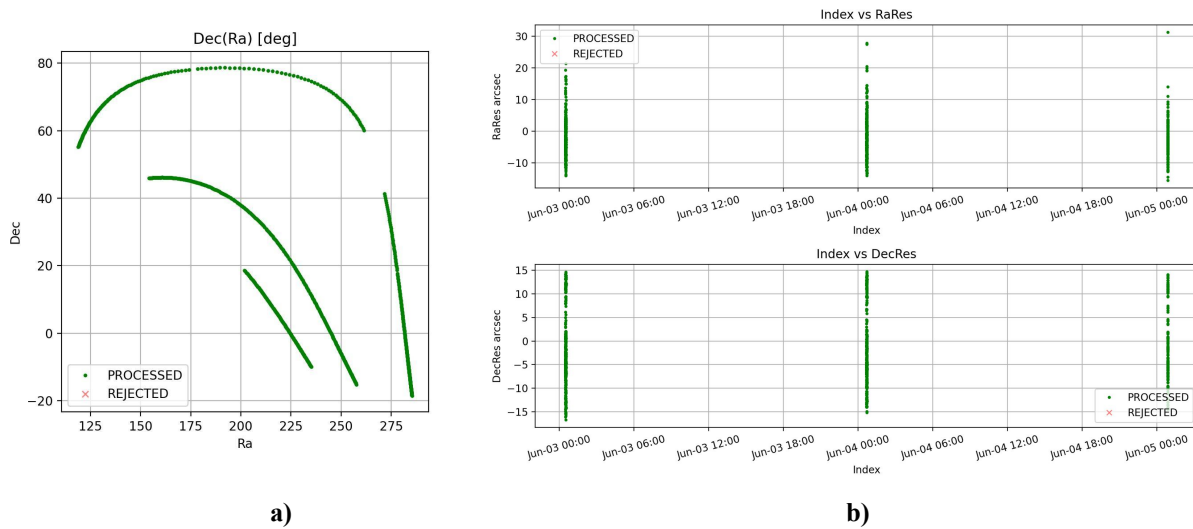


Fig. 8. a) Tracklets projection of the satellite no. 13153 on the plane right ascension/declination, b) residuals in the right ascension and declination obtained in the OD process using the LSQ method

Two independent software packages were used for the calculations: commercial ODTK [13] and in-house software based on Orekit libraries [14]. In addition, two different computational algorithms were used - calculations using ODTK were performed using the Kalman filter (KF), while software based on Orekit used the classical least square method (LSQ).

Orbital elements were determined along with *BC* estimation, and then propagation was performed to determine the predicted re-entry epoch. The results of the analysis are presented in Fig. 9.

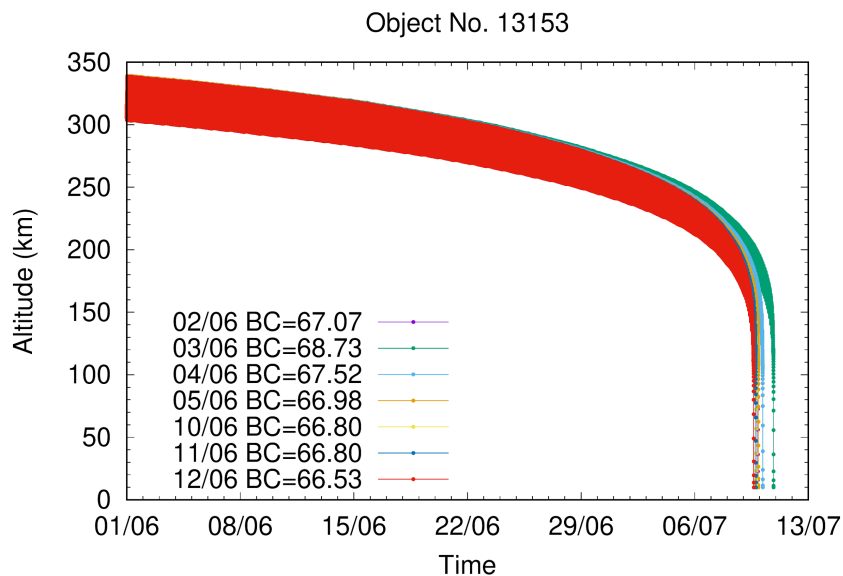
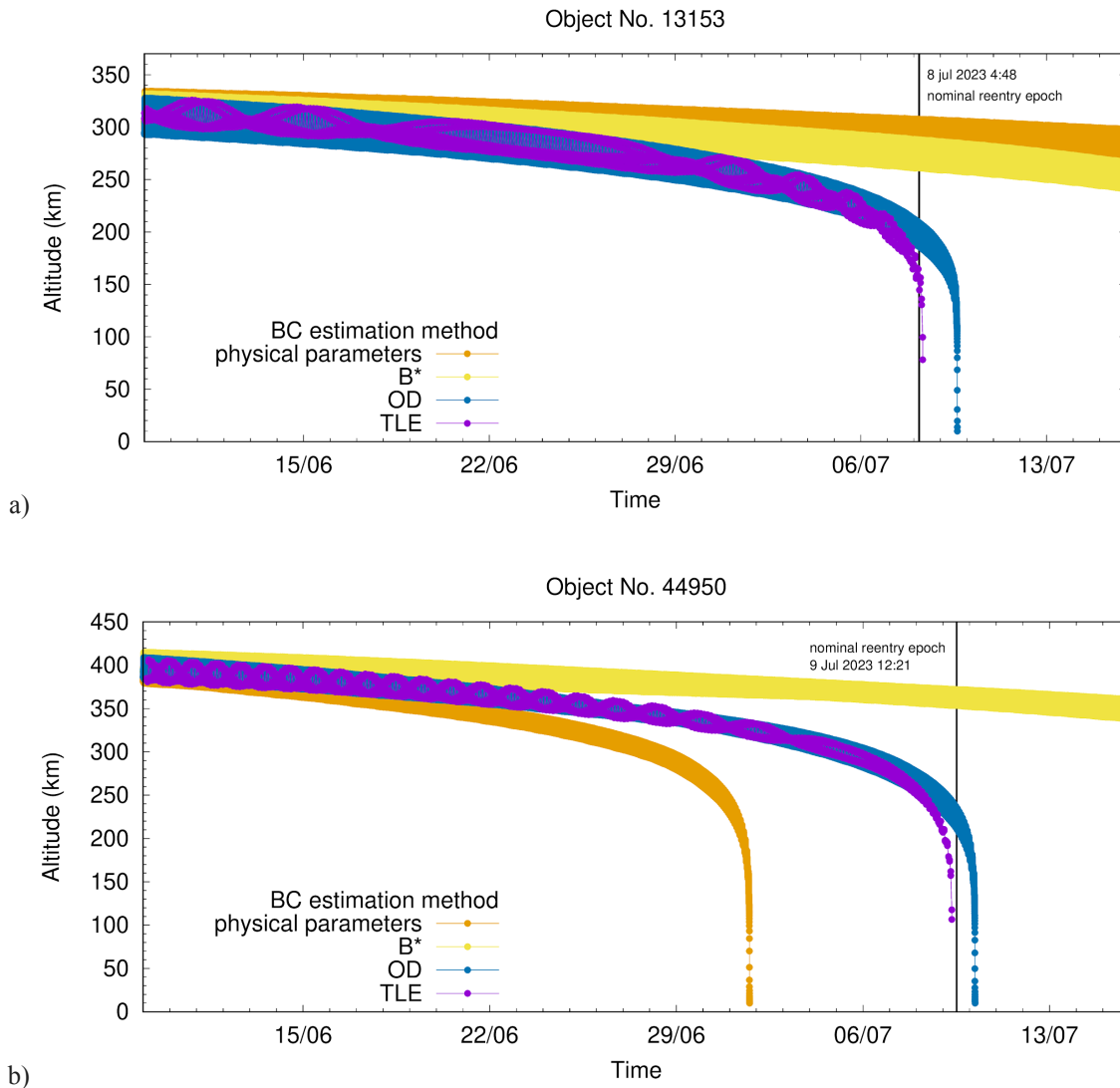
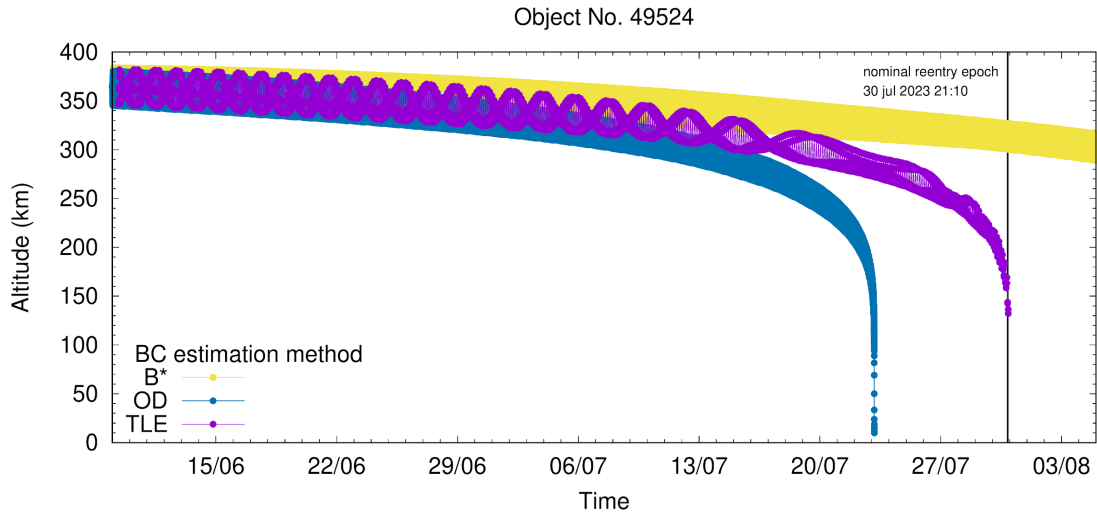


Fig. 9. Predicted altitude evolution before re-entry for COSMOS 1356 based on the OD calculations.

## 5. RESULTS

BC estimation using different methods leads to different values of this parameter. However, a direct comparison of the obtained numbers is not possible because the physical interpretation of the obtained results is not always the same. The estimation method may result in adding extra noise to this parameter which is impossible to separate. Therefore, in this paper, the comparison was carried out through estimation of the orbital parameters and its  $BC$  based on observational data (or TLE from the observation period), then propagating the orbit up to re-entry and comparing the predicted re-entry moment. For each method, a representative conversion example was selected and plotted in a common graph. The Fig. 10 shows the propagated height of the satellite above the earth's surface over time. The results obtained with different methods are plotted in different colors. The vertical line shows the nominal re-entry moment.





c) Fig. 10. Predicted altitude evolution before re-entry for a) COSMOS 1356, b) STARLINK-1125, c) COSMOS 1408 DEB based on four different  $BC$  estimation methods.

It can be seen that estimating the re-entry moment on the basis of previously known physical parameters or using the  $B^*$  coefficient is not very precise and should be used as a rough estimate.

Analysis using OD and fitting based on historical TLE allows the adjustment of parameters affecting the orbital motion of the satellite based on historical and current observational data. This significantly increases the accuracy of re-entry epoch prediction.

## 6. CONCLUSIONS

This paper shows the influence of various factors on the determination of the re-entry moment. The focus was on modeling the influence of atmospheric friction on the motion of the artificial satellite. In particular, it was shown how the choice of the atmosphere model and the adopted value of the ballistic coefficient affect the calculation process. The analysis carried out on the example of three satellites observed with the PST3 telescope showed that  $BC$  estimation is crucial for precise prediction of the moment of re-entry, and its determination must be based on observations.

In the future, it is necessary to broaden the analysis, e.g. cases where other types of observations will also be available. The development of algorithms related to determining the influence of atmospheric drag on the movement of an artificial satellite will improve the precision of modeling these events.

## 7. REFERENCES

- [1] Bowden, G. (2022). Orbit-localised thermosphere density prediction using a Kalman filter based calibration of empirical models. *Acta Astronautica*, 197, 6-13.
- [2] Bruinsma, S., Siemes, C., Emmert, J. T., & Mlynczak, M. G. (2022). Description and comparison of 21st century thermosphere data. *Advances in Space Research*.
- [3] Bruinsma, S., de Wit, T. D., Fuller-Rowell, T., Garcia-Sage, K., Mehta, P., Schiemenz, F., ... & Elvidge, S. (2023). Thermosphere and satellite drag. *Advances in Space Research*.
- [4] David J. G, Roberto A, Aleksander A. L. (2017) Ballistic coefficient estimation for reentry prediction of rocket bodies in eccentric orbits based on TLE data. *Mathematical Problems in Engineering*, Volume 2017, Article ID 7309637.
- [5] He, C., Yang, Y., Carter, B., et. al. (2018). Review and comparison of empirical thermospheric mass density models. *Progress in Aerospace Sciences*, 103, 31-51.

- [6] Kamiński K., Żołnowski M., Wnuk E., et. al. (2019). Low LEO optical tracking with small telescopes. Proceedings of the 1st NEO and debris detection conference, Darmstadt, Germany
- [7] Kaminski, K., Gołbiewska, J., Wnuk, E., et. al. (2022). Single and double pass optical LEO survey and tracking. 23rd AMOS Conference Proceedings, ISSN 2576-5965
- [8] Montenbruck O., Gill E. (2000). *Satellite Orbits - Models, Methods and Applications*. SpringerVerlag Inc., Berlin
- [9] Pardini C., Tobiska W. K., Anselmo L. (2006). Analysis of the orbital decay of spherical satellites using different solar flux proxies and atmospheric density models. *Advances in Space Research*, 37(2), 392-400
- [10] Pardini C., Anselmo L. (2008). Impact of the time span selected to calibrate the ballistic parameter on spacecraft re-entry predictions, *Advances in Space Research* 41(7), 1100-1114
- [11] Sang, J., Bennett, J. C., & Smith, C. H. (2013). Estimation of ballistic coefficients of low altitude debris objects from historical two line elements. *Advances in Space Research*, 52(1), 117-124.
- [12] Vallado, D. A. (2013). *Fundamentals of astrodynamics and applications* (4th ed.). Springer Science & Business Media
- [13] Vallado D. A, Hujsak R. S, Johnson T. M, et. al.(2010) Orbit determination using odtk version 6. ESA/ESAC astronomy centre, Madrid, Spain, 3-6
- [14] <https://www.orekit.org/>
- [15] Wnuk E. (1999). Recent progress in analytical orbit theories. *Advances in Space Research*, 23(4), 677-687. doi: 10.1016/S0273-1177(99)00148-9
- [16] Wnuk, E., 2015. STOP – The Short-Term Orbit Propagator. Kepassa 2015, 28–30 October 2015, Toulouse.